

Fault Behavior and Characteristic Earthquakes: Examples From the Wasatch and San Andreas Fault Zones

DAVID P. SCHWARTZ AND KEVIN J. COPPERSMITH

Woodward-Clyde Consultants, Walnut Creek, California

Paleoseismological data for the Wasatch and San Andreas fault zones have led to the formulation of the characteristic earthquake model, which postulates that individual faults and fault segments tend to generate essentially same size or characteristic earthquakes having a relatively narrow range of magnitudes near the maximum. Analysis of scarp-derived colluvium in trench exposures across the Wasatch fault provides estimates of the timing and displacement associated with individual surface faulting earthquakes. At all of the sites studied, the displacement per event has been consistently large; measured values range from 1.6 to 2.6 m, and the average is about 2 m. On the basis of variability in the timing of individual events as well as changes in scarp morphology and fault geometry, six major segments are recognized along the Wasatch fault. On the basis of the most likely number of surface faulting events (18) that have occurred on segments of the Wasatch fault zone during the past 8000 years, an average recurrence interval of 400-666 years with a preferred average of 444 years is calculated for the entire zone. Geologic data on the distribution of slip associated with prehistoric earthquakes and slip rates along the south-central segment of the San Andreas fault suggest that the M 8 1857 earthquake is a characteristic earthquake for this segment. Comparisons of earthquake recurrence relationships on both the Wasatch and San Andreas faults based on historical seismicity data and geologic data show that a linear (constant b value) extrapolation of the cumulative recurrence curve from the smaller magnitudes leads to gross underestimates of the frequency of occurrence of the large or characteristic earthquakes. Only by assuming a low b value in the moderate magnitude range can the seismicity data on small earthquakes be reconciled with geologic data on large earthquakes. The characteristic earthquake appears to be a fundamental aspect of the behavior of the Wasatch and San Andreas faults and may apply to many other faults as well.

INTRODUCTION

Paleoseismological studies, including exploratory trenching, mapping of tectonic geomorphic features, and morphometric analysis of fault scarps, are providing important basic information on the behavior of individual Quaternary faults. The goals of these investigations are to provide information on the interval between surface faulting earthquakes, the displacement during each event, slip rate, and fault segmentation. These parameters form the basis for developing estimates of the size of paleoearthquakes and fault-specific models of earthquake recurrence.

On the basis of displacement and recurrence data for past surface faulting events along the Wasatch fault zone, *Schwartz et al.* [1981] suggested that faults tend to generate essentially same size earthquakes having a relatively narrow range of magnitudes near the maximum. They referred to these earthquakes as characteristic earthquakes. A direct implication of the characteristic earthquake hypothesis is that the occurrence of earthquakes on individual faults and fault segments does not follow a log linear frequency-magnitude relationship of the form ($\log N = a - bM$) described by *Gutenberg and Richter* [1954].

The characteristic earthquake model, as defined above, is based on recently acquired paleoseismicity data. However, the concept that faults tend to generate essentially the same size earthquake is inherent in previous studies. *Allen* [1968] postulated that the historical behavior of the San Andreas fault may represent the long-term behavior as well, such that future large earthquakes will recur where they have in the past. The average earthquake "recurrence interval" concept [*Wallace*,

1970] is based on the assumption that the amount of slip that occurred in a past earthquake will reoccur and, when divided by the fault slip rate, will give the average recurrence interval between these same size events.

In the present paper we develop the concept of the characteristic earthquake by evaluating paleoseismicity data for the Wasatch and San Andreas fault zones. The data sets for these two zones are among the most extensive available for individual faults. These two faults occur within very different tectonic settings. The Wasatch fault zone lies in an intraplate environment that is characterized by generally low, and perhaps spatially and temporally variable, rates of stress release. The San Andreas fault is a major element of an interplate boundary that is characterized by high and generally uniform rates of stress release.

For each fault zone we discuss recurrence intervals, displacement per event, fault segmentation, and associated uncertainties in the context of how these parameters suggest marked similarity in the size of successive earthquakes. Earthquake recurrence based on the geological data is then compared with recurrence derived from the historical and instrumental seismicity data for each fault to determine the frequency of occurrence of the characteristic earthquake relative to earthquakes of other magnitudes. Finally, we discuss the implications of the characteristic earthquake model to fault behavior and earthquake generation.

WASATCH FAULT ZONE

The Wasatch fault zone (Figure 1) has not ruptured historically. However, detailed paleoseismologic studies at sites along the zone [*Swan et al.*, 1980; *Schwartz et al.*, 1983] have confirmed that it has generated repeated large-magnitude events in Holocene time and have yielded information on the timing and size of these events. On the basis of data from the first two

Copyright 1984 by the American Geophysical Union.

Paper number 4B0611.
0148-0227/84/004B-0611\$05.00

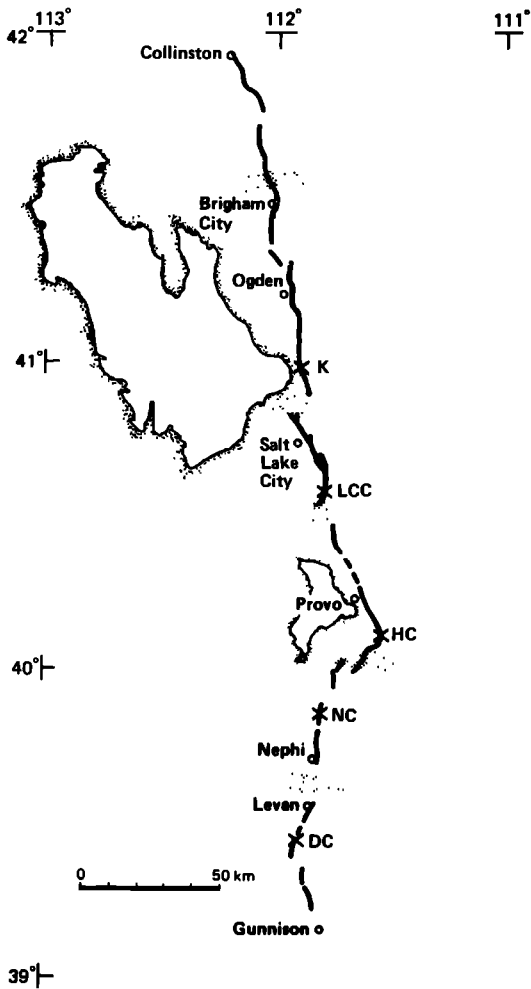


Fig. 1. Locality map for Wasatch fault zone. Sites described in the text are K, Kaysville; LCC, Little Cottonwood Canyon; HC, Hobble Creek; NC, North Creek; DC, Deep Creek. Stippled bands define proposed boundaries of major fault segments.

sites at Kaysville and Hobble Creek, *Schwartz et al.* [1981] proposed the characteristic earthquake model. Since then, data have been developed at sites along other parts of the zone. These allow an elaboration and further evaluation of this concept.

Geologic Basis for Number of Events and Displacement per Event on Normal Faults

Trenching of fault scarps along the Wasatch fault zone has shown that scarp-derived colluvium adjacent to the main fault can be used to quantify the number of past surface faulting events along normal faults. In trenches the colluvial stratigraphic sequence is commonly seen as stacked units or wedges that grade away from the main fault. The number of colluvial wedges is a basis for determining the number of events (Figure 2). Discrete colluvial wedges that represent individual past surface faulting events can be stratigraphically complex. Individual wedges are most clearly identified where a soil developed on a colluvial unit has subsequently been buried by colluvium derived from a younger faulting event. However, the occurrence of a soil, by itself, is not always indicative of an event, and multiple soils, especially thin organic A horizons, may develop within a single wedge in response to local conditions. The presence of infilled fissures that commonly form at the base of a scarp during surface faulting (Figure 2) are

also useful in defining wedges. The identification of individual fault-derived colluvial wedges may be less certain where they are distinguished only by textural or color changes. Along the Wasatch fault zone, the identification of individual event-derived wedges has been aided by tracing colluvial units laterally into faulted graben deposits that provide independent constraints on the sequence of faulting and deposition.

Estimates of the amount of displacement that occurred during past surface faulting earthquakes can be based on scarp morphology, topographic profiles of surfaces displaced across the fault, and, in trenches, the thickness of scarp-derived colluvial wedges. Once a single-event wedge is recognized, estimates of displacement can be made on the basis of the thickness of the wedge adjacent to the fault. Several factors affect the thickness and rate of colluvial deposition on the fault scarp free face. These include the initial slope of the faulted surface, the nature of the faulted materials, the local erosion or deposition occurring at the base of the scarp, and the cumulative height of the fault scarp. Because of these the thickness of the wedge will vary along strike of the fault. This variation can be seen, for example, along the trend of the 1915 Pleasant Valley fault scarp [Wallace, 1980]. Therefore the thickness of the wedge adjacent to the fault provides a minimum value of the height of the free face that was produced during a surface faulting event. In some cases, such as at the North Creek site on the Wasatch fault zone, the thickness of the wedge approximates the total scarp height.

Recurrence Intervals and Displacement per Event

Kaysville site. Recurrence at the Kaysville site (Figure 1) has been described in detail by *Swan et al.* [1980]. At Kaysville, at least three surface faulting events have displaced an alluvial fan during the past 8000 (± 2000) years. The basis for recognizing these three events is the occurrence of three colluvial wedges and correlative faulted and back-tilted graben deposits observed in trenches. Radiocarbon dating of charcoal from the graben indicates that the two youngest events have occurred within the past 1580 ± 150 ^{14}C years B.P., and stratigraphic and geomorphic relations suggest that the most recent event occurred within the past 500 years but prior to

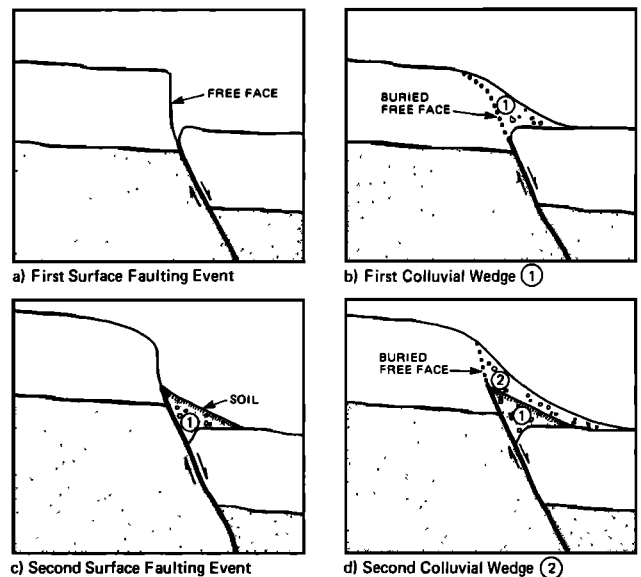


Fig. 2. Schematic diagram showing the development of colluvial wedges along normal fault scarps from successive surface faulting earthquakes.

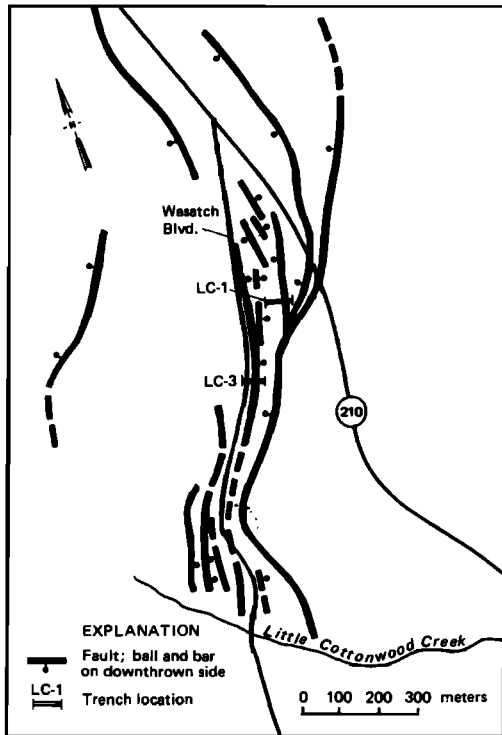


Fig. 3. Map of fault traces and trenches at the Little Cottonwood Canyon site.

settlement of the region in 1847. The best estimates of the interval between these events is 500–1000 years with the longer interval preferred.

At this location the net vertical tectonic displacement across the displaced alluvial fan is 10–11 m. The displacement for the two most recent events is well constrained and is similar. The older of these events was associated with back tilting in a fault sag that produced a free face along the main scarp with a minimum height of 3.5 m; the vertical tectonic displacement for this event is approximately 1.7 m. The most recent event produced a 4-m-high main scarp and a 2.2-m-high antithetic scarp for a net vertical tectonic displacement of 1.8 m.

These two events represent only one third of the cumulative scarp height at this location. While it is possible that the remaining 6.5–7.5 m of tectonic displacement could have occurred during the oldest event observed in the trench, it is

more likely that this displacement represents multiple events for which the evidence is below the base of the trench. If the displacements for the two youngest events are typical for this site, then displacement of the fan could have been produced by as many as five to six events.

Hobble Creek site. At the Hobble Creek site (Figure 1), six to seven surface faulting earthquakes have produced 11.5–13.5 m of vertical tectonic displacement during the past 13,500 years [Swan *et al.*, 1980]. The recognition of the oldest three to four events is based on the presence of strath terraces developed along Hobble Creek on the upthrown block of the fault. These events occurred in the period of time between the lowering of Lake Bonneville from the Provo level (about 13,500 years ago [Scott, 1980]) and the formation of a post-Provo pre-Utah Lake terrace (mid-Holocene) along the course of Hobble Creek. The three youngest events are defined on the basis of colluvial stratigraphy observed in trenches across a faulted alluvial fan that grades to the mid-Holocene surface. At Hobble Creek the number of post-Provo surface faulting events is well constrained, but because of the absence of dateable organic material the actual interval between events is not known. The average interval is in the range of 1700–2600 years. The morphology of the part of the scarp that represents the most recent event along this segment of the fault is more subdued than along the segment of the zone to the south, and the most recent event is estimated to have occurred at least 1000 years ago.

At the Hobble Creek site, actual displacements for the post-Provo events are not well constrained, and values for the average displacement per event range from 1.6 to 2.3 m for the six to seven events. On the basis of the log of trench HC-1 [Swan *et al.*, 1980] a minimum thickness of 2.75 m can be measured for a colluvial wedge associated with the event prior to the most recent event. An unknown amount of back tilting also occurred during this event. Therefore, while the tectonic slip for that event is uncertain, it appears to be compatible with the average values.

Little Cottonwood Canyon site. The estimation of recurrence and displacement per event at the Little Cottonwood Canyon site (Figure 1) is complicated by multiple fault traces and a wide, complex zone of deformation (Figure 3). Trenches were excavated across a major graben, the main east facing antithetic scarp, and the westernmost of three west facing scarps that define the main fault zone (Figure 3). The trenched

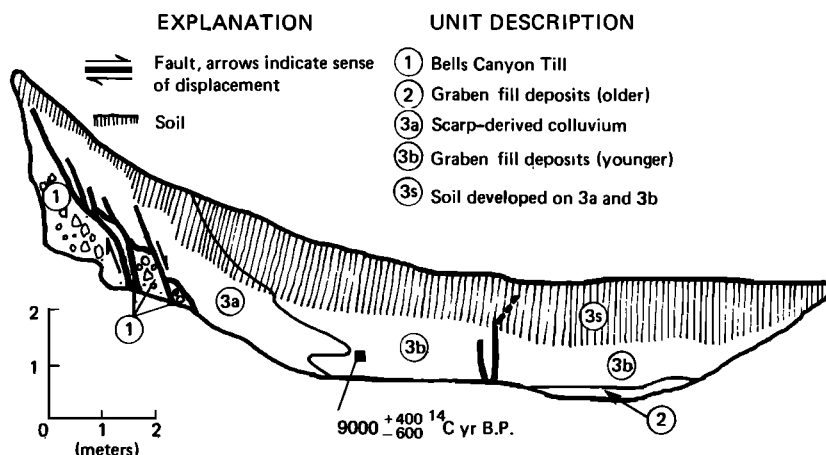


Fig. 4. Log of trench LC-3 (modified from Swan *et al.* [1981]) at the Little Cottonwood Canyon site.

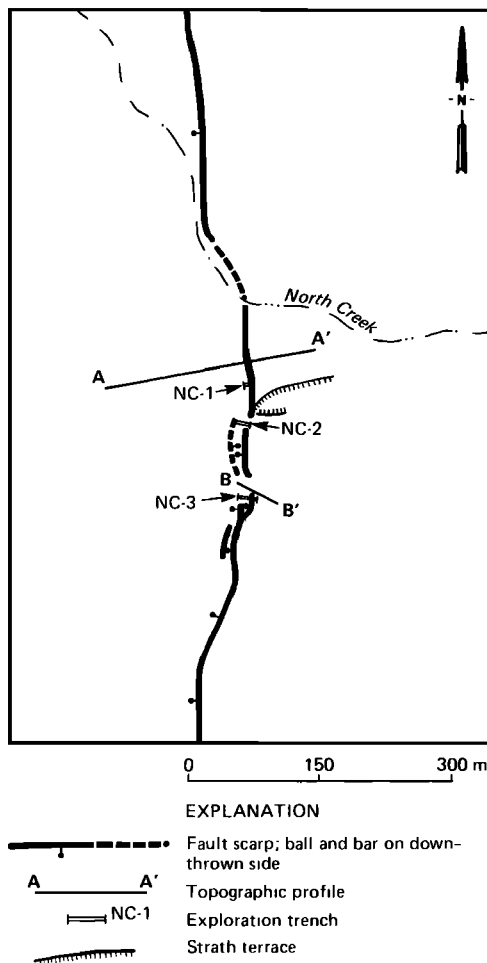


Fig. 5. Map showing the location of fault traces, strath terrace, trenches, and topographic profiles at the North Creek site.

scarp on the main fault is 4–4.5 m high, and the two scarps to the east have heights of 2 and 3.5 m. The trenches exposed Bonneville lake sediments, post-Bonneville alluvial fan and graben fill deposits, Bells Canyon till, and scarp-derived colluvium. Within the trenches, two events are recognized. Ra-

diocarbon dating using accelerator mass spectrometry on charcoal from trench LC-3 (Figure 4) has yielded preliminary dates of 9000 (+400; -600) ¹⁴C years B.P. for alluvium (unit 3b) that grades to scarp-derived colluvium (unit 3a) from the oldest event on the antithetic scarp. The alluvium has subsequently been faulted. Trench LC-1 (log not shown) crosses the westernmost splay of the main fault scarp. Accelerator dates of 7800 (+400; -600) and 8600 (+500; -400) ¹⁴C years B.P. were obtained for two charcoal samples from graben fill deposits in this trench. These deposits are correlative with alluvium (unit 3b) in trench LC-3 and have also been displaced during one event. The radiocarbon dates provide a minimum limiting age for the older faulting event. The younger event, the age of which is unconstrained, occurred after deposition of the charcoal-bearing alluvial deposits and prior to settlement of the region.

On the basis of a test pit and trench LC-1 on the east side of the graben, Swan *et al.* [1981] showed that the top of the Bonneville lake deposits is displaced approximately 13 m down to the west across the main fault exposed in the trench. On the west side of the graben the top of the Bonneville lake deposits is displaced about 9 m down to the east across the main antithetic fault. Therefore the tectonic displacement across the graben is about 4 m, and the average displacement for the two events in the trenches is 2 m per event.

The age dates and number of events from the trenches give a maximum average recurrence interval of ≥4000–4600 years. However, there are two other splays of the main fault scarp at this location for which there are no subsurface data, and it is uncertain whether they represent an additional two or three events. Swan *et al.* [1981] report a best estimate net vertical tectonic displacement of 14.5 m of the Bells Canyon moraine just south of the trench site. Using the net displacement, a displacement per event of 2 m, and an age for the moraine of 19,000 ± 2000 years gives an average recurrence interval of 2400–3000 years. Although the recurrence and displacement per event at this location are not nearly as well constrained as at other sites along the zone, the slip rate, late Quaternary net tectonic displacement, average displacement per event, average recurrence interval, and overall geomorphic development of the fault are similar to the Hobble Creek site and

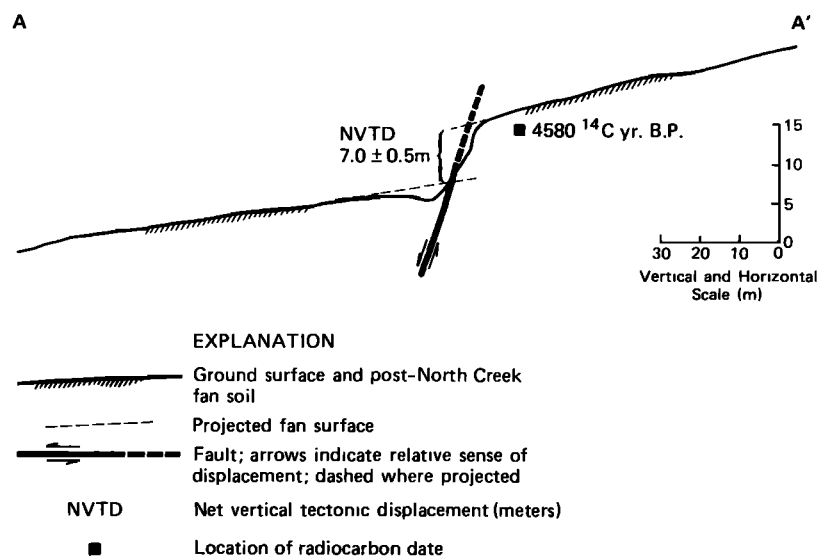


Fig. 6. Topographic profile across the displaced North Creek alluvial fan at the North Creek site.

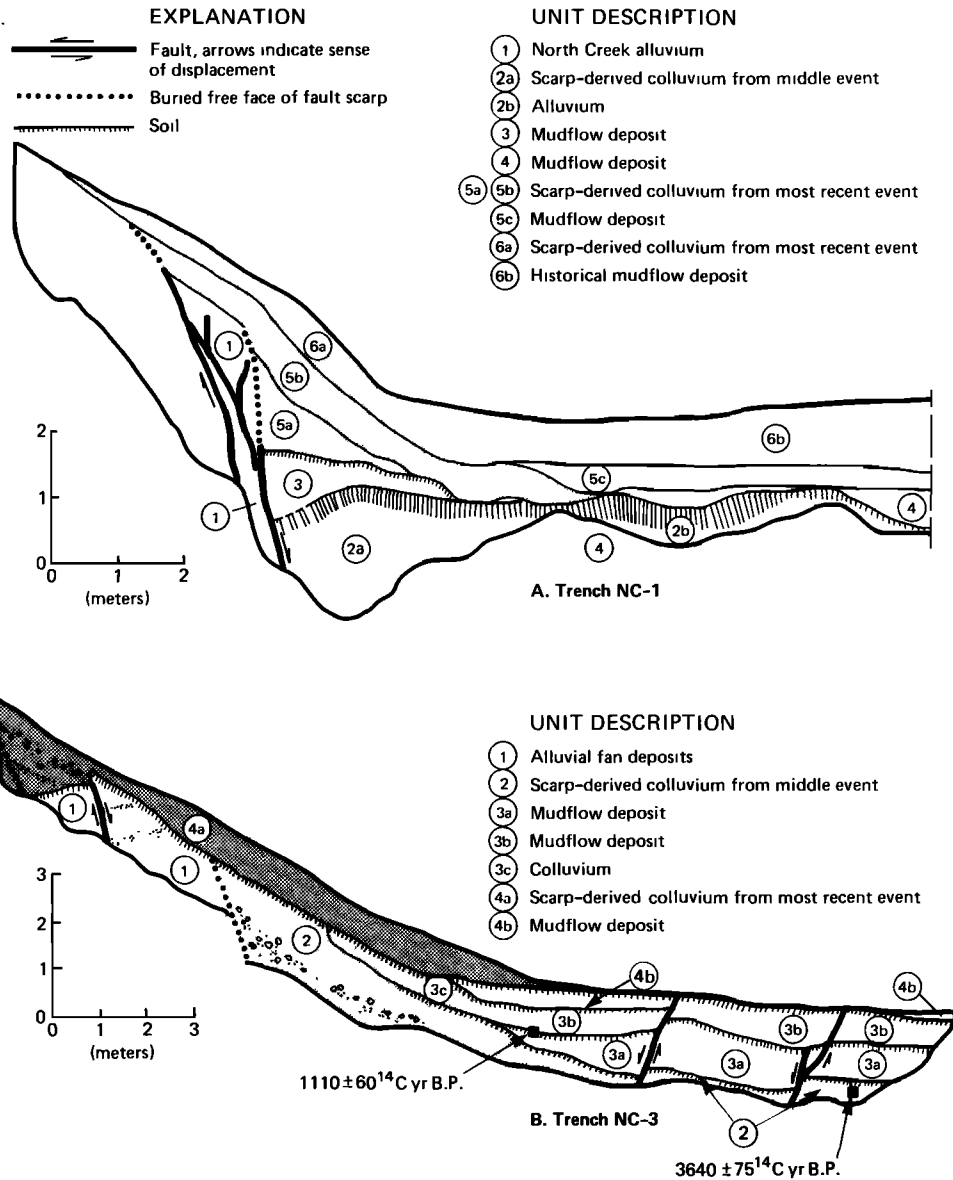


Fig. 7. Logs of trenches across the Wasatch fault zone at the North Creek site. (a) Trench NC-1. (b) Trench NC-3.

are compatible with data developed at other locations along the zone.

North Creek site. At North Creek (Figures 1 and 5) the fault displaces an alluvial fan that contains a burn layer dated at 4580 ¹⁴C years B.P. [Bucknam, 1978]. A topographic profile across the fan shows that its surface has been displaced 7 ± 0.5 m (Figure 6). This displacement is the result of three surface faulting events. The most recent event and the middle event are represented by scarp-derived colluviums (Figures 7a and 7b). An earlier surface faulting event is indicated by a strath terrace inset below the North Creek fan surface on the upthrown block of the fault (Figure 6).

The timing of the most recent event can be constrained by radiocarbon dates and scarp morphology. A date of 1110 ± 60 ¹⁴C years B.P. was obtained on charcoal from a displaced soil developed on a mudflow (unit 3a) in trench NC-3 (Figure 7b). In trench NC-2 (log not shown), deposits dated at 1350 ± 70 ¹⁴C years B.P. are displaced by the most recent event. These dates provide a maximum limiting age for the most recent event. The steep scarp angles measured along this segment of

the fault (42°), the lack of upstream migration of a knickpoint in a channel just above the fault scarp, and a generally continuous 15-km-long band that lacks vegetation and is coincident with the most prominent inflection on the scarp from the most recent event suggest very recent displacement, probably within the past 300–500 years.

Estimates of the amount of displacement that occurred during the most recent event at the North Creek site are based on the thickness of a scarp-derived colluvial wedge and topographic profiling of surfaces displaced across the fault. On the south wall of trench NC-1 (Figure 7a), displacement across the main western fault trace, which is based on the height of the buried fault scarp free face, is 1.9 m; the height of the free face associated with the eastern trace of the main fault is 0.5 m. This yields a total down-to-the-west displacement of 2.4 m. On the north wall, which was not logged, displacement occurred along a single fault plane, and the height of the buried free face was 2.2 m. Total displacement across antithetic faults observed in trenches NC-1 and NC-1A (not shown) is approximately 0.2 m down to the east. Subtracting the antithetic

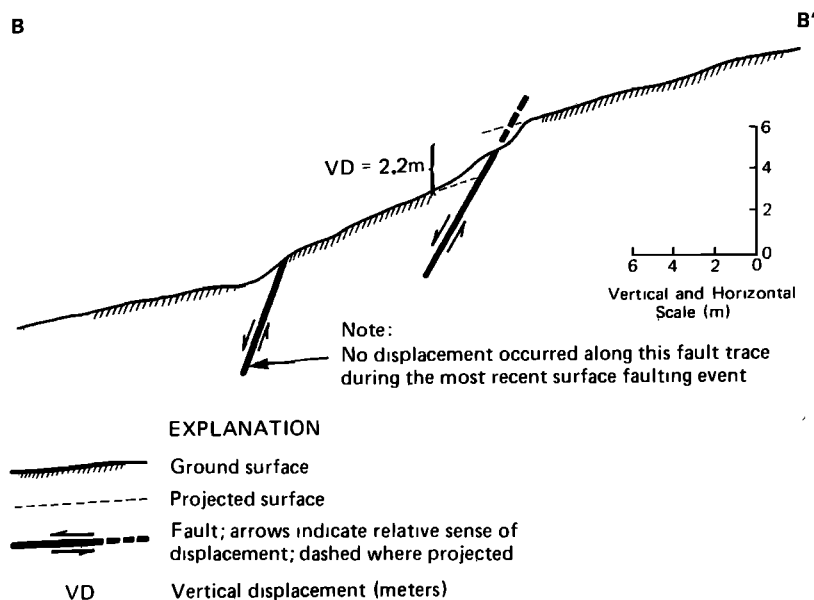


Fig. 8. Topographic profile across a mudflow displaced during the most recent event at the North Creek site.

displacement (0.2 m) from the estimates of displacement across the main fault (2.2 and 2.4 m) gives values of 2.0–2.2 m for the net vertical tectonic displacement across the zone. A topographic profile of the surface of a mudflow displaced across the fault near trench NC-3 (profile B-B', Figure 5) indicates a displacement of 2.2 m (Figure 8). This agrees well with the displacement value for the most recent event measured in trench NC-1.

Constraints on the timing of the middle event are obtained from radiocarbon dates on an organic-rich soil (Figure 7b) that formed on scarp-derived colluvium deposited following this event. The soil sample yielded conventional radiocarbon age dates of 3640 ± 75 ^{14}C years B.P., and the event occurred prior to this date.

Unit 2a in trench NC-1 (Figure 7a) and unit 2 in trench NC-3 (Figure 7b) are colluviums derived from the middle event. They have thicknesses of 2.5 and 2 m, respectively. These are minimum values because the bases were not exposed. However, as noted below, these values appear to approximate the displacement during this event. Relationships at trench NC-3 suggest very little, if any, back tilting during this event.

The oldest event is represented by a strath terrace that is inset below the North Creek alluvial fan surface and is preserved on the upthrown block of the fault above trench NC-1 (Figure 5). This terrace formed in response to the first event that displaced the North Creek fan. The height of the terrace scarp measured adjacent to the fault scarp is 2.6 m, and it approximates the displacement that occurred along the main fault trace during that event. Because of channel erosion that probably occurred in the vicinity of trench NC-1, scarp-derived colluvial units from this event may not have been preserved or may be below the bottom of the trench.

The well-constrained displacement of 2.0–2.2 m for the most recent event, the minimum values of 2–2.5 m for the middle event, and the 2.6 m for the oldest event give a cumulative slip of 6.6–7.3 m. This is essentially the same as the net vertical tectonic displacement of 7.0 ± 0.5 m for these three events indicated by the profile across the displaced North Creek fan (Figure 6). It suggests that the minimum values for the middle event are close to the actual displacement. Therefore, at this

location the past three events have had essentially the same size displacements in the range of 2.0–2.6 m.

Because of temporal variations in the radiocarbon content of atmospheric carbon dioxide, the conventional radiocarbon age dates used to calculate the actual intervals of time between faulting events have been corrected to calendar years using calibration tables of Klein *et al.* [1982]. The oldest and middle events occurred after 4580 ^{14}C years B.P. (charcoal in North Creek fan) and before 3640 ± 75 ^{14}C years B.P. (soil on scarp-derived colluvium in trench NC-3). These radiocarbon dates convert to a range of calendar dates of 3145–3510 B.C. and 1865–2295 B.C., respectively. This gives a maximum interval of 1645 years and a minimum interval of 850 years between the two dates, with the two events occurring between. If the most recent event occurred approximately 300–500 years ago, the interval between it and the middle event would be at least 3349–3979 years. The calculated average interval at this site ranges from 1700 to 2700 years. The 1700-year interval assumes that an event occurred immediately prior to the datum, which in this case is 5095–5460 years old. The 2700-year interval results if the oldest event immediately postdates the datum and the youngest event is very recent. In either case, actual intervals between events differ by a factor of 2 from estimates of the average interval at this site.

Deep Creek. Detailed subsurface investigations have not been made along the Levan segment of the fault. However, reconnaissance mapping between Levan and Gunnison indicates that only one surface faulting event has occurred along this segment since the early to middle Holocene. At Deep Creek (Figure 1) a single-event 2.5-m-high scarp displaces alluvial deposits dated by accelerator mass spectrometry at 7300 ± 1000 ^{14}C years B.P. At Pigeon Creek, 2 km to the north, the same scarp displaces an alluvial fan dated at 1750 ± 350 ^{14}C years B.P.

Summary. The recurrence and displacement per event data are summarized in Table 1 and illustrate several important aspects of the behavior of the Wasatch fault zone. Recurrence intervals vary along the length of the zone. Average intervals are shortest (1700–3000 years) along the four central segments between Brigham City and Nephi. In contrast, the ends are less active. A minimum interval of 5000 years occurred along

TABLE 1. Fault Behavior Data Wasatch Fault Zone

Segment	Site	Slip Rate, ^a mm yr ⁻¹	Displacement per Event, m		Recurrence		Elapsed Time, ^c years	Reference
			Measured	Average ^b	Interval	Average (yr)		
Collinston	...	≥ 0 (13,500)	≥ 13,500	this report
Ogden	Kaysville	1.3(+0.5, -0.2) ^d (8,000; +1000, -2000)	1.6	...	2 (after 1580) ^e	2000	≤ 500	Swan et al. [1980]; this report
Salt Lake City	Little Cottonwood Canyon	0.76(+0.6, -0.2) (19,000 ± 2000)	...	2 (2)	...	2400-3000	...	Swan et al. [1981]; this report
Provo	Hobble Creek	0.85-1.0 ^d (13,500)	2.7	1.6-2.3 (6-7)	6-7 (after 13,500)	1700-2600	> 1000	Swan et al. [1980]
Nephi	North Creek	1.27-1.36(±0.1) (4580) ^e	2.0-2.2 2.0-2.5	2.3 (3)	2 (between 4580 and 3640) ^e	1700-2700	300-500	this report
Levan	Deep Creek	≤ 0.35 ± 0.05	2.6 2.5	...	1 (after 1100) ^e 1 (after 7300) ^e	...	< 1750 ^e	this report

^aAge of displaced datum (years B.P.) on which slip rate is based is shown in parentheses.

^bNumber of events on which average is based is shown in parentheses.

^cTime in years since the most recent surface faulting earthquake.

^dModified from Swan et al. [1980].

^eAge in ¹⁴C years B.P. Standard deviation for each date is given in text.

the southern segment of the zone prior to its most recent event, and the northern segment has not had a recognized scarp-forming event during the past 13,500 years. Where radiocarbon dates constrain the actual interval between events, it is evident that the actual recurrence is not uniform and may vary from the average by at least a factor of 2.

Historical surface rupture on normal faults in the Basin and Range, for example, the 1915 Pleasant Valley, Nevada, fault scarp [Wallace, 1980], generally show systematic variation of displacement along the surface trace of the fault. For the Wasatch fault zone we do not know where individual trench sites are located with respect to past surface ruptures, and there is some uncertainty as to whether an individual measurement represents a minimum, a maximum, or an average displacement for that surface faulting event. Despite this the data clearly show that the displacement per event has been consistently large. Measured values range from 1.6 to about 2.6 m and the average displacement per event is about 2 m. The data indicate that displacements at the same location along the fault can be essentially the same during successive events.

The occurrence of successive large and similar displacement events is basic to the concept of the characteristic earthquake. An important point that must be considered is the threshold displacement that can be recognized as a discrete event in trenches or geomorphologically. Our experience suggests that for the Wasatch fault a displacement of 50 cm or larger along the main fault scarp should be recognizable. Under favorable geomorphic and stratigraphic conditions, significantly smaller displacements can be preserved and are recognizable. For example, antithetic faults with displacements of 20 and 21 cm that occurred during the most recent event at trench NC-3 at North Creek (Figure 7b) are observed as displaced stratigraphic horizons in the trench and are preserved as scarplets across the surface of an alluvial fan. While we cannot preclude the past occurrence of small (< 50 cm) displacement events, events with displacements between 50 cm and 1.5 m would be recognizable. However, we have not observed direct evidence of, or have been able to infer, the occurrence of these events in 17 trenches excavated across the zone.

Segmentation

A long (370 km) normal slip fault zone such as the Wasatch will only rupture for some fraction of its length during a sur-

face faulting event. The longest recorded surface rupture for a normal slip fault in the Basin and Range is 62 km for the 1915 Pleasant Valley earthquake (*M* 7 3/4). The 1983 *M_L* 7.1 Borah Peak, Idaho, earthquake ruptured approximately 40 km. The worldwide data on surface faulting along normal faults [Slemmons, 1977] show that rupture lengths of between 30 and 40 km are commonly associated with earthquakes in the magnitude range of 6.75-7.5. It is likely that future surface ruptures along the Wasatch zone will be in the 30-60+ km range. Given this, is the location of a future event random, or is the zone comprised of discrete segments that control the location and extent of rupture? If the latter is the case, can these segments be recognized? Using the range of values of historical surface rupture, Swan et al. [1980] suggested that the Wasatch fault zone consists of six to 10 segments, although individual segments were not specifically identified. On the basis of more complete paleoseismicity data, as well as new geophysical and geodetic data we believe that there is a sufficient basis for segmenting the fault zone, and we propose six major rupture segments. One area of uncertainty in the selection of segments is the degree to which data from a site can be used to characterize the behavior of a segment. A major site selection criterion during the Wasatch field studies was to choose sites that appeared to be representative of the section of the fault along which they were located, even though segmentation was not a primary consideration at the time. In addition, reconnaissance mapping has been done along the length of the zone in conjunction with the detailed site studies for the specific propose of extending and evaluating relationships beyond the individual trench sites. Therefore characterization of a segment, for example, its geomorphic development, is not based solely on a single location.

Proposed fault segments are shown on Figure 1. From north to south the segments, their length, and their orientation are (1) Collinston, ≥ 30 km, N20°W, (2) Ogden, 70 km, N10°W, (3) Salt Lake City, 35 km, convex east N20°E to N30°W, (4) Provo, 55 km, N25°W, (5) Nephi, 35 km, N11°E, and (6) Levan, 40 km, convex west. The identification of individual segments relies heavily on variability in the timing of individual events at locations along the entire fault zone (Table 1) as well as on changes in scarp morphology and fault geometry. The Collinston segment has had no identifiable surface faulting in the past 13,500 years. The Ogden segment has

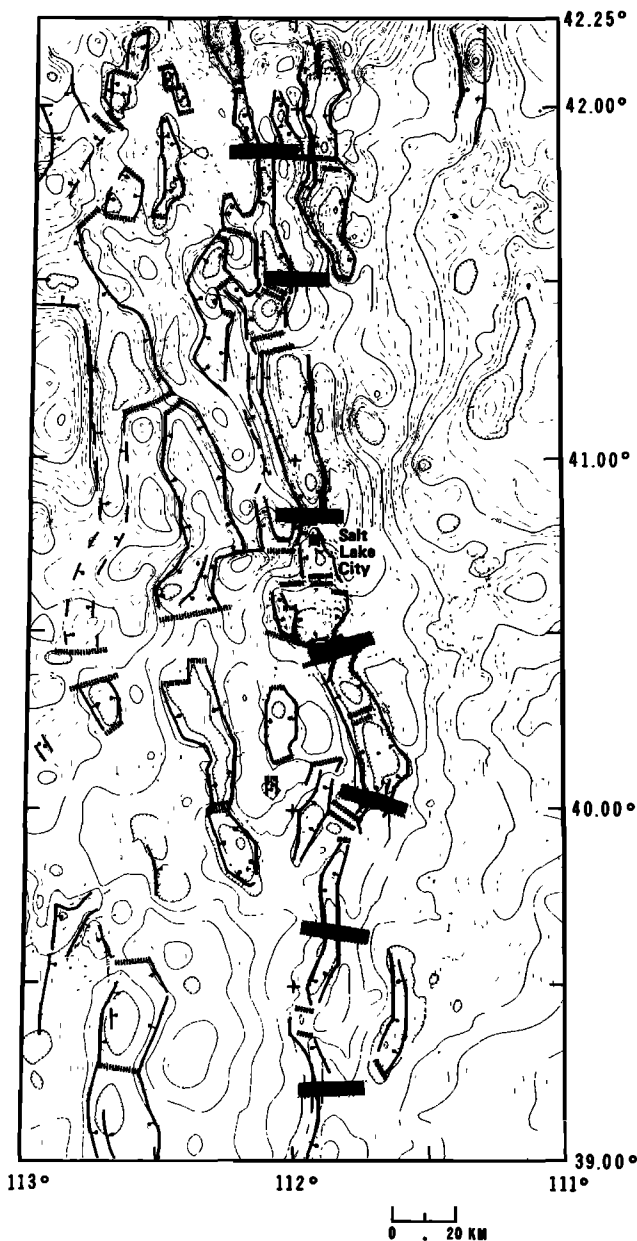


Fig. 9. Wasatch fault zone segment boundaries (stippled bands) superimposed on complete Bouguer gravity map. Gravity data, interpreted normal faults and basins (heavy lines with balls), and interpreted structural ridges or cross faults (double hachured lines) are from Zoback [1983].

experienced multiple displacements, including two within the past 1580 ^{14}C years B.P. and the most recent of these in the past 500 years. The Salt Lake City and Provo segments have each had repeated Holocene events. The timing of the most recent event along the Salt Lake City segment is uncertain, and the youngest event on the Provo segment appears to have occurred more than 1000 years ago. Along the Nephi segment, one event has occurred within the past 1100 ^{14}C years B.P. and probably as recently as 300–500 years ago, while two events occurred between 4580 and 3640 ^{14}C years B.P. The Levan segment has experienced only one event during the past 7300 ^{14}C years B.P., and this event occurred less than 1750 ^{14}C years ago.

Proposed segment boundaries are not sharply defined and may represent structurally complex transition zones a few to

more than 10 km wide. To varying degrees, boundaries selected on the basis of paleoseismic and geomorphic observations are coincident with changes in the trend of the fault, with major salients in the range front, with intersecting east-west structural trends observed in the mapped bedrock geology, with cross faults and transverse structural trends that occur at the ends of elongate basin-range blocks interpreted from gravity data [Zoback, 1983], and with geodetic changes [Snay *et al.*, 1984].

The boundary between the Collinston and Ogden segments is located at the northernmost extent of Holocene fault scarps along the range front. This boundary zone has no well-defined expression at the surface in the older structure, but it does occur in close spatial association with a cross fault at the southern end of a fault basin interpreted in the gravity data (Figure 9). The Ogden–Salt Lake City boundary occurs at the Ensign Peak salient, which is coincident with a major structural and lithologic change that occurs where the northeast to east-northeast trending northern boundary of the Uinta uplift crosses the northwest Wasatch front trend [Hintze, 1980]. It has expression as an east-west structure in the gravity and also defines the southern end of a basin-range block (Figure 9). On the basis of triangulation and trilateration surveys, Snay *et al.* [1984] suggest that prior to 1978 the section of the Ogden segment between Salt Lake City and Ogden was exhibiting compressional strain, while at the same time the Salt Lake City segment was undergoing extension. They also note that a diffuse east-west pattern of seismicity is associated with the Ensign Peak salient and conclude that this salient is a boundary separating distinct segments of the fault. The Salt Lake City–Provo segment boundary is well expressed in the gravity data (Figure 9) and occurs at a major salient in the range front. This salient occurs where the Charleston–Nebo thrust, which defines the southern boundary of the east-northeast trending Uinta uplift, intersects and extends across the north-northwest Wasatch trend [Hintze, 1980]. The Provo–Nephi boundary occurs where the fault zone changes strike from $\text{N}20^\circ\text{W}$ to $\text{N}10^\circ\text{E}$, the active trace is expressed as an echelon steps, and there is a clear difference in the timing of the most recent event across the boundary zone. This is a broad boundary that is generally coincident with a northwest trending cross fault that defines the southern end of an elongate fault block (Figure 9). The Nephi–Levan boundary is not well expressed in the gravity data; however, it occurs at the intersection of the Nebo thrust with the Wasatch front and an abrupt change in lithology from Paleozoic metasediments and carbonates to Jurassic–Paleogene shallow marine and fluviolacustrine sedimentary rocks. In addition, it represents a 17-km-long break in the continuity of Holocene surface faulting.

The Wasatch fault zone segments proposed above are based on data that represent the behavior of the fault zone in post-Provo (13,500 years) time. An important question is to what degree do these represent long-term, or permanent, fault segments? Figure 10 is a north-south topographic profile along the crest of the Wasatch Range. It is, in effect, an expression of the long-term slip history along the entire fault zone. Proposed segment boundaries based on geologic and geophysical data have been superimposed on the profile, and they are generally coincident with distinct changes in the height of the range. Using only the profile to select segments, it is possible to select alternative boundaries. This is partially an effect of slight profile distortion resulting from changes in the strike of the range along its length. The most marked changes occur where the height of the range steps up across the Collinston-

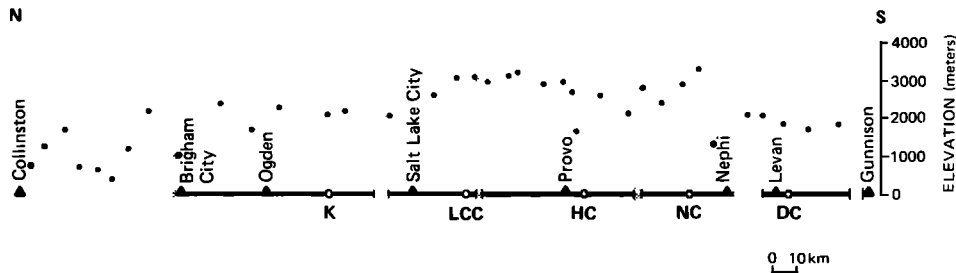


Fig. 10. North-south topographic profile along the crest of the Wasatch Range. Stippled bands are segment boundaries from paleoseismological and geophysical data superimposed on the profile. Open circles are trench sites and localities discussed in the text: K, Kaysville; LCC, Little Cottonwood Canyon; HC, Hobble Creek; NC, North Creek; DC, Deep Creek. Solid line along base of profile defines the lateral extent of post-Provo (13,500 years) surface faulting.

Ogden and Nephi-Levan boundaries. Slip rates are lowest on these end segments (Table 1). The height of the range increases across the Ogden-Salt Lake City segment boundary and drops off slightly as the Provo-Nephi boundary is approached. Slip rates for the Salt Lake City and Provo segments are roughly comparable. The height of the range decreases sharply across the Nephi-Levan boundary. Holocene fault scarps also decrease in height toward the southern end of the Nephi segment and die out coincident with the drop in range elevation.

Implicit in the description of the fault segments is the concept that each segment defines a distinct rupture segment during a surface faulting earthquake. We cannot exclude the possibility that some ruptures have crossed segment boundaries or that adjacent segments have ruptured completely during the same event. However, the compatibility of the rupture segments based on the paleoseismicity data with the variation in the height of range suggests that the proposed segments for the Wasatch fault zone have generally behaved as discrete units through a significant period of time. The boundaries would then represent zones that may act as barriers to rupture propagation. Their location appears to be defined, in large part, by transverse structures. These could serve to decouple adjacent segments.

Recurrence for the Zone Based on Geological Data

Swan *et al.* [1980] suggested an average recurrence interval along the entire Wasatch fault zone of 50–430 years. This was calculated by using the minimum (500 years) and maximum (2600 years) intervals estimated at Kaysville and Hobble

Creek, respectively, and assuming that these were representative of six to 10 independent fault segments. As discussed above, however, the fault zone is most likely composed of six segments, the recurrence interval between segments can be significantly different, and the recurrence for a given segment can vary significantly.

On the basis of these new data and the behavioral variability they indicate, we feel that a more realistic estimate of the average recurrence for the zone can be obtained by using the number of events recorded in the geological record along each segment of the fault during a particular interval. A difficulty in evaluating recurrence for the zone in this manner is that there is no single datum common to all segments for which there is a complete paleoseismic record. Table 2 summarizes the number of events and average recurrence intervals for the zone. The number of events actually observed at each site and the datum are given. The age of the datum is based on either radiocarbon dating or correlation. It can be seen that although the ages of the datums differ, three of the sites have records post 7300–9000 ¹⁴C years B.P., Kaysville has an 8000-year history, and a mid-Holocene terrace at Hobble Creek provides a datum for at least the past approximately 6000 years. On this basis, we have selected 8000 years as the interval over which to calculate an average recurrence for the zone. The number of events observed at each site during this interval are given. The 12–13 events listed give an average recurrence interval of 615–666 years for the zone during this period of time. We consider this a maximum average recurrence interval. As discussed previously, the geological data indicate

TABLE 2. Number of Surface Faulting Earthquakes and Average Recurrence Intervals for the Wasatch Fault Zone

Segment	Site	Events Postdatum at Site		Minimum Number of Events Post-8000 ^a	Probable Number of Events Post-8000 ^a
		No.	Age		
Collinston	...	≥ 0	13,500 ^a	0	0
Ogden	Kaysville	≥ 3	8,000 ^a	3	5
Salt Lake City	Little Cottonwood Canyon	≥ 2	7,800–9,000 ^b	2	4
Provo	Hobble Creek	6–7	13,500 ^a	3–4	4
Nephi	North Creek	3	4,580 ^b	3	4
Levan	Deep Creek	1	7,300 ^b	1	1
Total				12–13	18
Average recurrence interval, years				615–666	444

^aAge in years B.P.

^bAge in ¹⁴C years B.P.

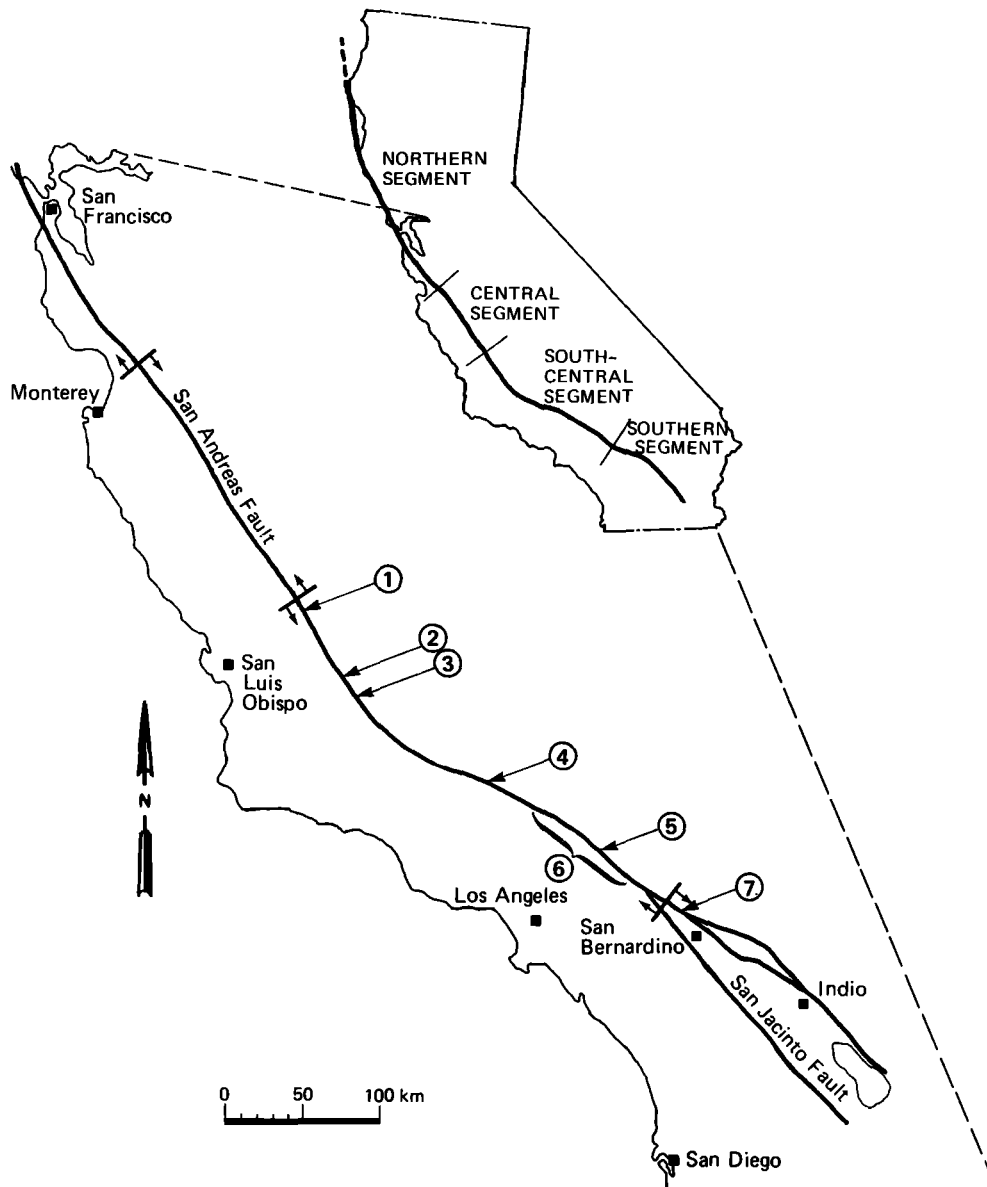


Fig. 11. Location map of the south-central segment of the San Andreas fault. Individual localities are the following: 1, Bitterwater Valley; 2, Wallace Creek; 3, Van Matre Ranch; 4, *Rust* [1982*b*] locality; 5, Pallett Creek; 6, Lake Elizabeth to Wrightwood; 7, Lost Lake.

that the number of events observed at Kaysville and Little Cottonwood Canyon are clearly minima. Also, within the 8000-year period, it is likely that additional events have occurred at Hobbles Creek and North Creek. Our best estimate of the number of events at each locality during the past 8000 years is given. The total of 18 events yields an average recurrence interval of 444 years. This value represents a preferred average recurrence for the zone. If additional events have not been recognized, the average recurrence interval will be somewhat shorter. The addition of two events lowers the average recurrence to 400 years. On this basis, we consider 400–666 years to be a reasonable range for the average recurrence interval of a surface faulting earthquake along the entire Wasatch fault zone.

SAN ANDREAS FAULT ZONE

Allen [1968] recognized differences in historical behavior of various parts of the San Andreas fault zone (Figure 11) and identified four segments: a northern segment that was the lo-

cation of the 1906 rupture, a central segment that is presently creeping and has been the location of repeated moderate earthquakes during the this century, a south-central segment that was the location of the 1857 rupture, and a southern segment that has not generated large earthquakes during the historical period. *Allen* [1968] suggested that the historical behavior of these segments may represent their longer-term past and future behavior as well; that is, the segments that have generated large earthquakes will continue to do so, and the creeping segment will continue to generate frequent moderate earthquakes.

Recent work on the San Andreas fault has led some investigators to develop further the concept of consistent behavior of segments of the San Andreas fault over geologic time periods. *Sieh* [1981] proposed two alternative models for the distribution of slip associated with large earthquakes on the south-central segment. One of these, termed the "uniform earthquake" model, is based on the assumption that the distribution of slip associated with the 1857 earthquake is typical of the distribution during previous events. *Rust* [1982*a*] present-

ed evidence for repeated similar size offsets in the central part of the big bend of the San Andreas fault and postulated that uniform behavior of the segment may span several earthquake cycles over the past thousand years. *Bakun and McEvilly* [1979, 1984] have studied in detail a series of six earthquakes that occurred on the southern part of the central segment of the San Andreas fault over the past 125 years, including the 1966 Parkfield earthquake. Because the earthquakes appear to be very similar in size and seismologic characteristics, *Bakun and McEvilly* [1984] conclude that they represent characteristic earthquakes for this segment.

Geologic data regarding the distribution of slip associated with prehistoric earthquakes and fault slip rates have been gathered for the south-central segment of the San Andreas fault. The observations of the rupture length and the distribution of fault slip associated with the 1857 earthquake provide an excellent basis for comparing geologic data on prehistoric earthquakes to determine whether previous events along this segment were of essentially the same size as the 1857 earthquake. To assess the significance of the observations that have been made, several possible models of fault behavior associated with large earthquakes are first considered.

Fault Displacement Models

Three possible models of displacement associated with large earthquakes are shown diagrammatically in Figure 12. In each model the displacements associated with individual earthquakes are plotted cumulatively along a specific reach of a fault. The implications of each model in terms of observational data are also presented.

The first model, called a variable slip model, allows earthquakes of variable size (slip distribution) to occur randomly along the fault. At any point along the fault this behavior is expressed as variable amounts of displacement associated with each of a series of earthquakes. Because of the lack of permanent segments the fault will tend, through time, to distribute slip evenly along its length such that long-term slip rates will be essentially the same at any point along the fault. A full distribution of earthquake sizes, perhaps best described by a log linear frequency magnitude relationship with $b \approx 1$, would be expected to characterize the behavior of the fault.

The uniform slip model, first named by *Sieh* [1981], introduces an element of nonrandom behavior in that a large earthquake that is assumed to have essentially the same slip distribution occurs periodically along the same segment of the

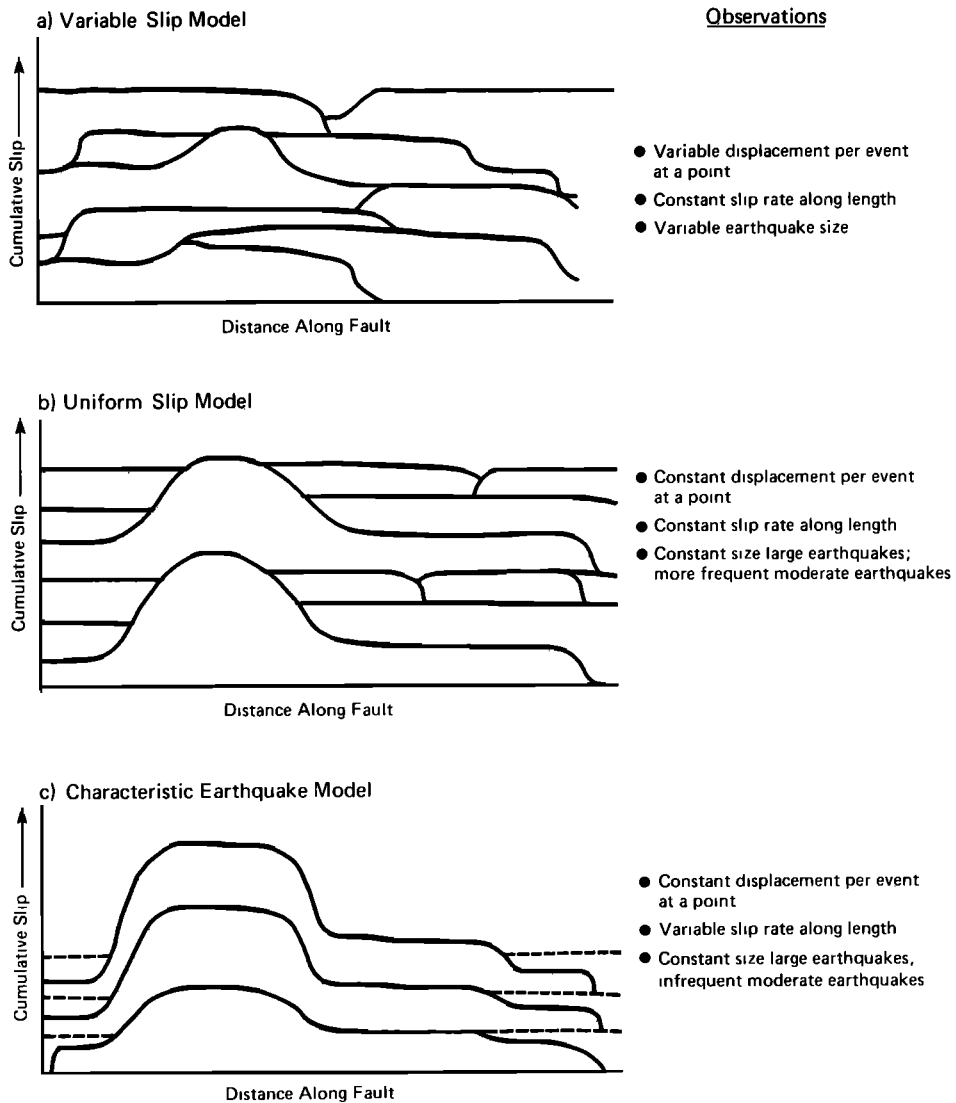


Fig. 12. Diagrammatic representation of three models of displacement associated with large-magnitude earthquakes. The cumulative slip distribution is illustrated for each model, and the implications of each model relative to observational data are given. Dashed lines represent ruptures from adjacent segments.

TABLE 3. Displacement per Event for the South-Central Segment of the San Andreas Fault

Locality	Displacement per Event, ^a m	Reference
1	3.5	<i>Sieh</i> [1978a] and <i>Sieh and Jahns</i> [1984]
2	3.5 9.5 ± 0.5 12.3 ± 1.2 11.0 or 11.7 ± 2.2	<i>Sieh and Jahns</i> [1984]
3	8 8 10	<i>Sieh</i> [1981]
4	7-7.5 7-7.5 7-7.5	<i>Rust</i> [1982b, 1983]
5	2 2 0.8-1.5 0.7-1.3	<i>Sieh</i> [1984]
6	3-4.5 2.5-4 3-5	derived from <i>Sieh</i> [1978a]

^aDisplacement listed in order of increasing age; the first value is the 1857 displacement; values reflect precision given by each investigator.

fault. Those parts of the rupture that experience relatively small amounts of slip in the large earthquake experience more frequent moderate displacement events that allow them to catch up. This model implies that the cumulative slip and the slip rate along the length of the fault should be essentially constant and that at a point along the fault the displacement associated with individual events should be essentially constant (Figure 12). Because moderate earthquakes occur more frequently than large events according to this model, a log linear frequency-magnitude relationship may characterize earthquake recurrence along the segment.

The characteristic earthquake model is based on the assumption that the distribution of slip associated with the characteristic event along a fault segment is repeated in successive events. In a manner similar to the uniform earthquake model the single-event displacements at any point along the fault are essentially constant. However, because the original slip distribution is repeated in successive earthquakes, the slip rate will vary along the length of the fault. The variation in slip rate should be systematic, with high rates occurring where the largest displacements occur. As shown in Figure 12, some overlap of rupture with adjacent segments may occur toward the ends of the segment. For this model to apply, overlap should be insufficient to equalize the cumulative slip along the segment. The characteristic earthquake model implies a non-linear earthquake frequency-magnitude relationship that is dominated by the characteristic event and that has a low *b* value in the moderate-magnitude range.

In order to classify the behavior of the south-central segment of the San Andreas fault into one of the models described above, the data regarding the distribution of slip associated with individual events and fault slip rates are summarized below. Earthquake recurrence data for this segment are presented in the following section.

Displacement per Event and Fault Slip Rate

Displacement as a function of location along the south-central segment has been well documented for the 1857 earthquake [*Sieh*, 1978a]. Amounts of displacement are variable along the segment, and although the maximum is about 9.5 m, the average is about 4 m. In order to assess the constancy of

the slip distribution, displacement per event data for the south-central segment have been compiled in Table 3. All of the displacement estimates, except those made for Pallett Creek (locality 5), are based on measured stream channel offsets. In most cases, several stream offsets have been measured along a limited reach of the fault in order to arrive at an average offset associated with any single event. For example, *Rust* [1982b, 1983] examined offset stream channels over a 30-km-long section of the fault centered on locality 4 (Figure 11) in order to arrive at an average value of 7-7.5 m for the three most recent events. At Pallett Creek (locality 5) the estimates of displacement per event are based on a detailed investigation of offset geologic units and small-scale structural features within the fault zone [*Sieh*, 1984]. Near Wallace Creek (locality 2), preliminary examination of stream gully offsets [*Sieh*, 1977] suggests that at least two events, each having about 12 m of displacement, occurred prior to those listed in Table 3, although these have not yet been thoroughly documented. It is apparent from the displacement data that at a particular point along the fault the amount of slip associated with repeated earthquakes is remarkably constant. This observation provides a basis for rejecting the variable slip model and for favoring either the uniform slip or the characteristic earthquake model.

If the 1857 slip distribution has been repeated through several seismic cycles as required by the characteristic earthquake model, then significant differences in the slip rate at various points along the fault segment should be observed. As summarized in Table 3, the single-event displacements along the Carrizo Plain section of the segment (localities 2 and 3) are about 1.5 times those to the south at locality 4 (Figure 11) and are about 2.5 times those along the southern part of the segment (locality 6); the slip rates would be expected to reflect a similar relative difference. The slip rate estimates are summarized in Table 4, including the time periods over which the rates have been calculated. The slip rates presented for localities 4 and 6 are based on a combination of displacement per event data and age correlations presented by *Sieh and Jahns* [1984]. For example, at locality 6 the cumulative slip that has occurred in the past approximately 800 years (post event R) is 13 m and in the past 500 years (post event T) is 11 m [*Sieh and Jahns*, 1984].

Comparison of the slip rate and displacement data indicates that the localities displaying high slip rates (the northern part of the segment) are also associated with large displacements

TABLE 4. Slip Rates for the South-Central Segment of the San Andreas Fault

Locality	Slip Rate, ^a mm yr ⁻¹	Time Period, years	Reference
2	33.9 ± 2.9 35.8 (+5.4, -4.1)	4,000 13,000	<i>Sieh and Jahns</i> [1984] <i>Sieh and Jahns</i> [1984]
4	19-22 ^b	800-1000	
5	9 ^c	1,100	<i>Sieh</i> [1984]
6	17-21 ^d	500-800	
7	25	9,400	<i>Weldon and Sieh</i> [1980] and <i>Sieh</i> [1983]

^aValues reflect precision given by each investigator.

^bSlip rate based on displacement data of *Rust* [1982b, 1983] and age correlations of *Sieh and Jahns* [1984].

^cAn additional 10 mm yr⁻¹ may have occurred as warping [*Sieh*, 1984].

^dSlip rate based on displacement data of *Sieh* [1978a] and age correlations of *Sieh and Jahns* [1984].

during the most recent surface faulting events. The slip rate at Wallace Creek (locality 2) is about 1.5 times the rate near the central part of the segment (locality 4) and is up to 2 times the rate along the southern part of the segment (locality 6). We feel that this systematic variation in slip rate, which reflects the distribution of slip associated with the 1857 earthquake, favors the characteristic earthquake model rather than the uniform slip model.

The slip rate data are not well enough distributed along the south-central segment to assess directly the detailed variations in rate along its length. However, between locality 2 (in the Carizzo Plain) and locality 4 (just south of the big bend) a significant decrease occurs. This stretch of the San Andreas fault coincides with a major change in the complexity of the San Andreas fault system. North of the big bend most of the interplate deformation is accommodated on the San Andreas fault. Within and south of the big bend, much of the interplate strain is accommodated by major strike-slip branch faults and by the reverse faults and folds of the Transverse Ranges.

Significant differences in slip rate along strike have been documented elsewhere along the San Andreas fault zone. A very similar decrease in slip rate occurs where the central segment of the San Andreas splays north into the complex system of faults in the San Francisco Bay region. The slip rate along the central segment is $32 \pm 2 \text{ mm yr}^{-1}$, as determined geodetically [Lisowski and Prescott, 1981]. Along the northern segment south of the San Francisco, the slip rate measured geodetically is only $12.2 \pm 3.9 \text{ mm yr}^{-1}$ [Prescott et al., 1981; W. H. Prescott and S. B. Yu, unpublished manuscript, 1984] and geologically is also about 12–13 mm yr^{-1} [Hall, 1984]. The location of this twofold to threefold decrease in slip rate on the San Andreas fault coincides with the major change in the structural complexity of the fault system.

Some uncertainty exists regarding the accuracy of the slip rates estimated at various points along the south-central segment. At Wallace Creek (locality 2), detailed studies of the geologic history and displacements of stream gulleys crossing the fault constrain the rate to $33.9 \pm 2.9 \text{ mm yr}^{-1}$ during the past 3700 years [Sieh and Jahns, 1984]. By dividing this slip rate into the individual displacements associated with pre-1857 events at Wallace Creek, Sieh and Jahns [1984] estimate the timing of these prehistoric earthquakes and suggest correlations with some of the events identified at Pallett Creek to the south (locality 5). The sequence of displacements at various localities along the segment defines the 1857 event and several previous events. In addition, the age constraints at Wallace Creek and Pallett Creek provide a means of estimating the age of these paleoearthquakes and correlating displacements at other locations along the segment. For example, at locality 4, three distinct 7- to 7.5-m events have been recognized by Rust [1982b, 1983], and Sieh and Jahns [1984] suggest that these events correlate with the three most recent events at Wallace Creek (the 1857 earthquake, event V, and event R). On the basis of this correlation, the slip rate at locality 4 over the 1012-year period following event F and preceding 1857 [Sieh, 1984] is about $22 \text{ m} \div 1012 \text{ years} = 22 \text{ mm yr}^{-1}$. This slip rate is significantly lower than the 34 mm yr^{-1} at Wallace Creek. For the slip rate at locality 4 to be higher than this the events identified at locality 4 would need to be younger than those at Wallace Creek, implying that some displacement events occurred at locality 4 but are unrecognized at Wallace Creek. There is no indication in the displacement data for additional events between Wallace Creek and locality 4.

Along the southern part of the segment (locality 6), which includes Pallett Creek, a series of 3- to 5-m events have been identified and correlated with dated events at Pallett Creek [Sieh and Jahns, 1984]. These displacements and age estimates provide the basis for the slip rate of 17–21 mm yr^{-1} given in Table 4. At the Pallett Creek site itself (locality 5), Sieh [1984] has found that individual displacements are only about 1–2 m and that the slip rate is only 9 mm yr^{-1} . Sieh [1984] suggests that the displacements and slip rate may be anomalously low at this location because the Pallett Creek site lies near the end of an en echelon segment. The consistently higher displacement values both immediately to the north and to the south of Pallett Creek also argue that Pallett Creek values may be anomalous. Nevertheless, the slip rate along the southern part of the segment (19 mm yr^{-1}) is significantly less than that at Wallace Creek (34 mm yr^{-1}). In order for the slip rate within locality 6 to match that at Wallace Creek, the identified displacements at locality 6 would have to be considerably younger than proposed by Sieh and Jahns [1984]. This would imply that the prehistoric record of earthquakes at Pallett Creek is missing several events over the past thousand years. However, Sieh [1984] argues that it is unlikely that any large earthquakes, especially those that may have occurred in the past thousand years or so, have escaped detection at the Pallett Creek site. The conclusion, therefore, is that the slip rate is indeed lower along this section of the fault than at Wallace Creek.

At Cajon Creek (locality 7), which lies just south of the 1857 rupture, the slip rate averaged over the past 9400 years has been about 25 mm yr^{-1} [Weldon and Sieh, 1980; Sieh, 1983]. Just to the north of this site, the San Jacinto fault joins the San Andreas fault. It can be argued that to the north of this junction the slip rate on the San Andreas fault should be the sum of the individual rates to the south. The slip rate on the San Jacinto fault has varied by an order of magnitude over the past 730,000 years [Sharp, 1981]. To compare meaningfully and sum the slip rates on the San Jacinto and San Andreas faults, comparable time periods must be considered. During the period from 6000 to 400 years B.P., which compares reasonably to the 9400 years B.P. to present time period used at Cajon Creek, the slip rate on the San Jacinto fault was 1.4–2.0 mm yr^{-1} [Sharp, 1981]. Therefore, during this time period the San Jacinto fault added very little to the San Andreas slip rate of 25 mm yr^{-1} north of their junction. Although the seismic slip rate from major historical earthquakes during the period 1890–1973 suggests that the rate on the San Jacinto fault has increased to as high as 8 mm yr^{-1} [Thatcher et al., 1975], the slip rate over a comparable period of time has not been determined on the San Andreas fault south of its junction with the San Jacinto fault. It is quite possible, as proposed by Sharp [1981], that the San Andreas and San Jacinto faults alternate in assuming dominant roles in accommodating interplate motion. Thus periods of high rates of slip on the San Jacinto fault may coincide with periods of low rates on the San Andreas fault and vice versa [Sharp, 1981].

The displacement-age correlations presented by Sieh and Jahns [1984] suggest that toward the ends of the characteristic 1857-type ruptures some overlap occurs with other events to the south (e.g., locality 6) and possibly also to the north. However, there is no evidence in the displacement data that rupture from these other events propagates into the central part of the segment, and the slip rate data confirm that even in the areas of overlapping ruptures such as locality 6, the displacements are not sufficiently large to equalize the cumula-

tive slip and rates of slip along the south-central segment.

Although the southern stretch of the segment (locality 6) appears to be a zone of overlap between 1857-type earthquakes to the north and other events to the south, the southern extent of the latter events is not known. On the basis of stratigraphic relationships near Indio, *Sieh* [1983] concludes that the most recent large earthquake occurred on the southern segment more than 560 years ago. This suggests that at least the two most recent pre-1857 events recognized at locality 6 did not rupture as far south as Indio.

DISCUSSION

The characteristic earthquake model is related to the size and likelihood of occurrence of earthquakes that a fault generates, and therefore it has direct implications for the frequency of occurrence of earthquakes of various magnitudes. As summarized previously, the characteristic earthquake model implies that characteristic events dominate earthquake recurrence, resulting in nonlinear frequency-magnitude relationships having low b values in the moderate-magnitude range. It should be possible to test this implication against observations of earthquake recurrence. Both geologic and seismicity recurrence data are available for the Wasatch and San Andreas fault zones. The geologic data, which span time periods long enough to include several seismic cycles, provide information on the recurrence intervals between characteristic earthquakes. The seismicity data, which do not include complete seismic cycles for either the Wasatch or the San Andreas faults, constrain the rate of occurrence of smaller-magnitude events. A comparison of the two types of recurrence data is used to illustrate the implications of the characteristic earthquake model to fault-specific recurrence relationships.

Comparison of Seismologic and Geologic Recurrence

Wasatch fault zone. The historical and instrumental seismicity data for the Wasatch Front region, which contains the Wasatch fault, have been the subject of extensive study [*Arabasz et al.*, 1979, 1980; *Arabasz and Smith*, 1981]. The following discussion draws heavily on the results of these studies but is focused on the seismicity that is directly related to the Wasatch fault.

The historical record began in about 1850, and regional network instrumental data have been available since about 1962. The epicenter locations for the period from 1850 to 1950 are based primarily on felt reports, and the locations for the period from 1950 to 1962 are chiefly locations determined by the U.S. Coast and Geodetic Survey [*Arabasz et al.*, 1980]. The largest earthquakes that could have been associated with the Wasatch fault are the intensity *MM* VII (M_L 5.5) 1910 and 1914 earthquakes. *Arabasz et al.* [1980] estimate that the historical seismicity catalog is complete for Modified Mercalli epicentral intensity $I_0 \geq VIII$ since 1850; $I_0 \geq VII$ since 1879; $I_0 \geq VI$ since 1939; and $I_0 \geq V$ since 1950. Therefore the apparent absence of earthquakes of intensity VIII or greater along the Wasatch fault zone during the approximately 134-year historical period is probably real and not the result of an incomplete earthquake catalog.

The locations of epicenters based on instrumental records for the period 1962–1978 are presented by *Arabasz et al.* [1980]. The Wasatch front seismic network was established by the University of Utah in mid-1974 at which time the resolution increased greatly. A diffuse pattern of epicenters and clusters of epicenters generally occurs along the Wasatch front area. In detail, however, the local area close to the Wasatch

fault (less than 20 km either side of the fault) is characterized by a distinctly low level of seismicity. This paucity of small-magnitude earthquakes along the fault was noted by *Smith* [1974], who called attention to two 70-km-long zones along the fault north and south of Salt Lake City that have been persistently quiescent since at least 1962. *Arabasz et al.* [1980] postulate that these zones may be seismic gaps for earthquakes larger than magnitude 3 since 1962 and probably since at least 1955.

Along some parts of the Wasatch fault zone, for example, north of Brigham City and south of Nephi, small-magnitude earthquakes can be spatially correlated with the fault. At other locations, such as near Salt Lake City and north of Nephi, clusters of earthquakes are occurring 10–30 km west of the fault, and some of these events may, depending on the down-dip geometry of the fault, be associated with the Wasatch fault. Surface mapping and trench exposures indicate that the fault dips at the surface an average of about 60°–70° to the west. If this geometry persists to seismogenic depths (4–12 km), then the epicenters that lie farther than about 5–7 km to the west of the surface trace are probably not associated with the fault. Recent interpretations of deep seismic reflection profiles across the Wasatch and some other faults of the Basin and Range province [*Zoback*, 1983; *Smith and Bruhn*, this issue] suggest that the dips of some of these normal faults may decrease with depth (i.e., become listric). However, assuming that the Wasatch fault is listric, the steep dips at the surface and the constraints on the probable maximum depths of seismicity of about 8–12 km [*Arabasz and Smith*, 1981] indicate that the seismicity plotted more than 15–20 km west of the fault is not occurring on it.

The seismicity to the east of the Wasatch fault zone is spatially associated with the East Cache fault in the Logan area. To the south of this area, no throughgoing Quaternary fault has been found east of the Wasatch fault, but the seismicity may be controlled by pre-Cenozoic structure [*Arabasz et al.*, 1980] or by bending stresses related to crustal flexure [*Zandt and Owens*, 1980].

To examine the recurrence relationships for the instrumental seismicity (1962–1983) on the Wasatch fault zone, we have selected a relatively narrow corridor that extends 20 km west to 10 km east of the fault. The frequency-magnitude plot of these data is shown in Figure 13. The baseline over which the recurrence relationship is constructed is only 1.5 magnitude units. However, for a somewhat larger region that is centered on the Wasatch fault *Arabasz et al.* [1980] arrive at very similar b values. For data from July 1962 to June 1978 the maximum likelihood estimate of b value at the 95% confidence limit is 0.95 ± 0.15 [*Arabasz et al.*, 1980].

The recurrence estimates for surface faulting earthquakes along the entire Wasatch fault zone based on geologic data are represented in Figure 13 by a box that shows the range of uncertainty in recurrence intervals and magnitude. The range in recurrence intervals is 400–666 years. The moment magnitude of surface faulting earthquakes is estimated on the basis of the segment lengths (35–70 km), down-dip fault width (7–12 km), and average displacement per event (2 m). Using the moment magnitude relationship $M_0 = 1.1M_L + 18.4$ proposed for the Utah region by *Doser and Smith* [1982], the range of magnitudes is about 7–7.5.

The most striking feature of the recurrence relationship (Figure 13) is the distinct absence of moderate-magnitude earthquakes (M 5.5–6.5) during the 21-year period of instrumental record. This is in agreement with the previous 112-year

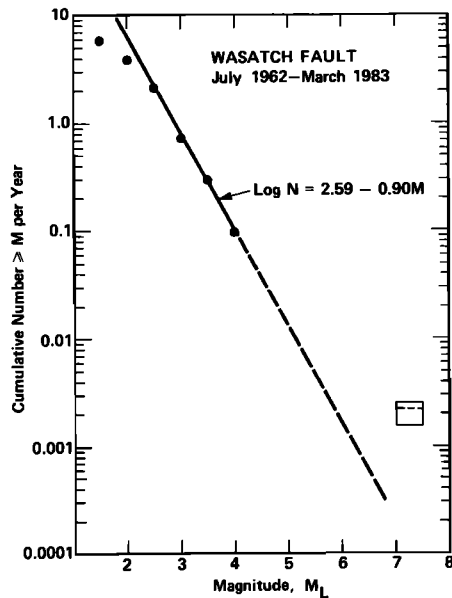


Fig. 13. Cumulative frequency-magnitude plot of instrumental seismicity for the period July 1962 to March 1983 along a zone containing the Wasatch fault. The 370-km-long zone extends approximately 20 km to the west of the fault and 10 km to east. The dashed portion of the recurrence relationship is a linear extrapolation. The box represents the range in recurrence intervals (400–666 years) and magnitudes (7–7.5) based on the geologic data. The preferred recurrence interval estimate of 444 years is indicated by a dashed line within the box.

historical period (1850–1962), which contains no earthquakes larger than intensity VII (approximately M 5.7) within a corridor extending 50 km west and 25 km east of the Wasatch fault. A linear extrapolation of the recurrence curve from the smaller magnitudes assuming a constant b value leads to underestimates of the frequency of large earthquakes. Only by assuming a lower b value in the moderate-magnitude range (M 5.5–6.5) can the seismicity recurrence be reconciled with the geologic recurrence. The paucity of moderate events in the seismicity record along the fault zone is in agreement with the geologic observations that suggest an absence of displacement events smaller than the characteristic event. The seismicity data are regional, while the geologic data have been gathered at particular points along the fault. The agreement between the seismicity data and geologic data suggests that the low b value in the moderate-magnitude range reflects the true behavior of the fault and is not merely a result of “point” rather than “entire fault” observations of paleoseismic events, as has been suggested by *Anderson and Luco* [1983].

The primary conclusion that can be drawn from the analysis of the seismicity data and a comparison with the geologic recurrence data is that the Wasatch fault zone as a whole tends to generate characteristic earthquakes having magnitudes of 7–7.5 and that moderate magnitude (M 5.5–6.5) events occur infrequently (at least apparently so from the time sample of seismicity during the last century). Geologic observations at particular points along the fault support the repeated occurrence of similar size events. Presumably, then, individual segments of the fault generate their own characteristic earthquakes. The size of these events may differ somewhat between individual segments but appears to be about M 7–7.5 for the segments studied.

San Andreas fault zone. Since the 1857 earthquake (moment magnitude M 8), the south-central segment of the San Andreas fault has been associated with low levels of seis-

micity. This marked quiescence is documented in the historical and instrumental seismicity records. During the period from 1857 to 1900 the historical record is complete for magnitudes greater than 6.0–6.5 [*Topozada et al.*, 1980]. Besides the aftershocks to the 1857 earthquake, only one earthquake was reported along the south-central segment during this time period, which occurred on February 2, 1881, and had an estimated magnitude of 5.6 [*Topozada et al.*, 1980].

The historical and instrumental seismicity data for the post-1900 period were compiled for a 40-km-wide strip centered on the south-central segment of the San Andreas fault from the catalog by *Real et al.* [1978] and from the California Institute of Technology catalog. The 1952 Kern County and the 1971 San Fernando main shocks and aftershocks were excluded from the catalog. The earthquake catalog for this zone appears to be complete for $M \geq 5$ –5.5 for the period of 1900–1931 and is complete for $M \geq 3.5$ –4 for the period 1932–1980. A frequency-magnitude relation was developed for the post-1900 seismicity data and is presented in Figure 14.

Also shown in Figure 14 is a box that represents the geologic estimates of the recurrence intervals and magnitudes of 1857-type earthquakes on the south-central segment. *Sieh and Jahns* [1984] estimate the recurrence of large earthquakes at Wallace Creek by dividing the displacement associated with the three most recent surface faulting earthquakes by the late Holocene slip rate. The result is three intervals that range from 240 to 450 years, and this range is represented in Figure 14 by the range in number of events. A magnitude range of 7.5–8 (moment magnitude) is assumed for these events, which is appropriate to the seismic moment estimated for the 1857 event by *Sieh* [1978a] and to previous events that appear to have the same rupture length and slip distribution.

As is the case for the Wasatch fault, the most pronounced feature of the frequency-magnitude relationship (Figure 14) is

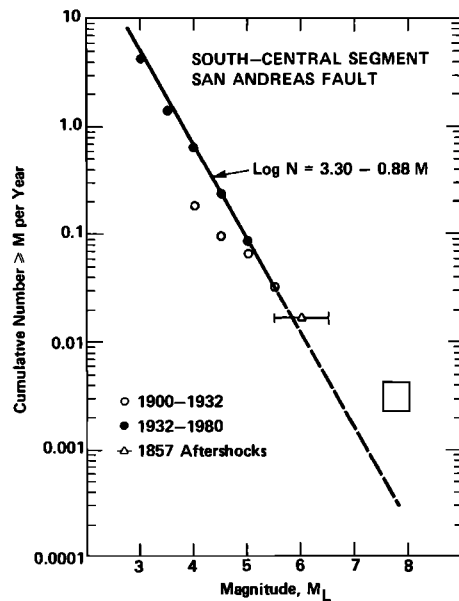


Fig. 14. Cumulative frequency-magnitude plot of instrumental seismicity for the period of January 1900 to December 1980 along a zone containing the south-central segment of the San Andreas fault. The 360-km-long zone is centered on the fault and extends 20 km either side of it. Aftershocks of the 1952 Kern County and the 1971 San Fernando earthquakes were excluded from the catalog. The dashed portion of the recurrence curve is a linear extrapolation. The box represents the range in average recurrence intervals (240–450 years) and moment magnitudes (7.5–8) based on the geologic data.

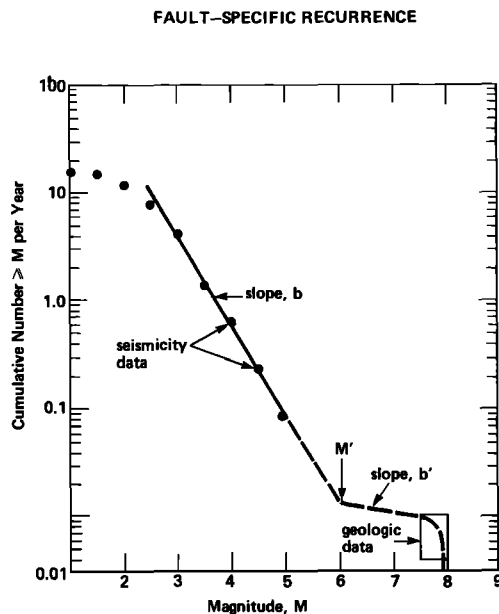


Fig. 15. Diagrammatic cumulative frequency-magnitude recurrence relationship for an individual fault or fault segment. Above magnitude M' a low b value (b') is required to reconcile the small-magnitude recurrence with geologic recurrence, which is represented by the box.

the mismatch between the position of the recurrence curve based on seismicity data and the recurrence of large events based on geologic data, reflecting a near absence of moderate-magnitude (M 6–7) earthquakes. This is in agreement with the scarcity of moderate magnitude events during the 43-year (1847–1900) historical period. A very low b value is required in this moderate-magnitude range to reconcile the data throughout the range of magnitudes.

Implications

The conclusion to be drawn from the preceding analysis of the earthquake recurrence data for the Wasatch and San Andreas faults is that log linear recurrence relationships having a constant b value may not be appropriate for individual faults or fault segments. Linear extrapolation of the recurrence relationship from the lower magnitudes tends to underestimate the frequency of occurrence of the large, characteristic events. A match between the recurrence of smaller magnitudes ($b \approx 1.0$) and larger magnitudes requires a very low b value (0.2–0.4) in the moderate magnitude range. This implies that the characteristic earthquakes are occurring at the expense of the moderate-magnitude events. This does not mean that moderate-magnitude events smaller than the characteristic earthquake never occur on individual faults or fault segments; rather their frequency of occurrence is less than would be expected by a recurrence curve passing through the characteristic magnitude and having $b \approx 1.0$. It should be emphasized that this type of recurrence behavior is pertinent only to individual faults and fault segments and not to regions. Constant b value recurrence models have been well documented on a worldwide basis and for large regions, which usually contain a number of individual faults.

A significant implication of the characteristic earthquake model to recurrence estimation is that additional parameters besides a and b values are required to characterize fault-specific recurrence (Figure 15). The slope of the recurrence curve (b') must be defined in the moderate-magnitude range,

and the magnitude (M') at which the change in slope occurs must be identified. These parameters can be determined directly from historical seismicity data if the record is sufficiently long or by including geologic estimates of recurrence.

Recurrence relationships of the type shown in Figure 15 have been documented by *Báth* [1981, 1983] in Turkey and Greece. Along the Mexican coast [*Singh et al.*, 1981, 1983] and coastal Alaska [*Purcaru*, 1975; *Lahr and Stephens*, 1982], segments of subduction zones show lower b values for larger earthquakes, suggesting a tendency toward the generation of a characteristic earthquake. *Singh et al.* [1983] argue that this occurs because individual segments of the zone, which are relatively permanent through time, have constant dimensions and generate essentially the same size earthquake. *Wesnousky et al.* [1983] make the same arguments for faults in Japan.

It has been argued that foreshocks and aftershocks may contribute significantly to the total number of events within an earthquake cycle and may be sufficient in number to increase the number of moderate size events such that a linear frequency-magnitude relationship results at the completion of a full cycle [*Anderson*, 1983]. However, studies of the 1857 earthquake indicate that it was accompanied by two moderate foreshocks ($5 \leq M \leq 6$), which most likely occurred on the adjacent central segment [*Sieh*, 1978b], and by only two large aftershocks (M 6) that were large enough to be widely felt [*Agnew and Sieh*, 1978; *Sieh*, 1978b]. The two aftershocks have been included in the frequency-magnitude plot in Figure 14. In addition, *Singh et al.* [1983] have documented a similar nonlinear frequency-magnitude relationship along segments of the Mexican subduction zone that have experienced two full cycles of major earthquakes with associated foreshocks and aftershocks. We conclude that it is unlikely that the foreshocks and aftershocks of the characteristic earthquake are sufficient to fill in the frequency-magnitude relationship such that a constant b value relationship results.

The characteristic earthquake model also has significant implications for assessments of seismic hazard associated with a particular fault or fault segment. Estimates of the likelihood of occurrence of large earthquakes based on extrapolation of the frequency of occurrence of small earthquakes may be subject to considerable error. Likewise, the concept of a "probable" earthquake that is somewhat more likely to occur than the maximum event and therefore is usually assumed to be somewhat smaller, may also be erroneous. In reality, the characteristic earthquake, which is probably also the maximum event, may be more likely to occur than a smaller, noncharacteristic earthquake. Methods such as those proposed by *Anderson* [1979] and *Molnar* [1979] that develop fault-specific recurrence relationships on the basis of fault slip rate and a constant b value may tend to overestimate the frequency of moderate earthquakes and underestimate the frequency of large events.

The physical basis for the generation of characteristic earthquakes is not well understood. The data presented for the Wasatch and San Andreas faults suggest that each tends to maintain fixed scales over repeated seismic cycles. That is, rupture segments, barriers to fault rupture, and the distribution of slip appear to persist through repeated earthquakes. *Aki* [this issue] argues that this type of self-similar behavior can be observed in the detailed seismologic characteristics of repeated earthquakes. Likewise, it can be argued that the constitution and strength of fault zone materials as well as the style of stress application can be considered essentially constant through several seismic cycles. Given that this set of

conditions remains relatively constant, we would expect generally uniform behavior of the fault with respect to the size of the characteristic earthquake that it produces.

The characteristic earthquake model appears to define the behavior of the Wasatch fault zone and south-central San Andreas fault zone, each of which has an extensive geological and seismological data base. We feel that the characteristic earthquake is a fundamental aspect of fault behavior and may apply to many other faults as well.

Acknowledgments. Much of the data presented in this paper is the result of a 5-year study of the Wasatch fault funded by the Earthquake Hazards Reduction Program of the U.S. Geological Survey. F. H. Swan III and K. L. Hanson played key roles in these studies and contributed to discussions regarding the characteristic earthquake hypothesis. R. R. Youngs suggested ways of testing the implications of the hypothesis relative to earthquake recurrence data. W. J. Arabasz graciously provided the earthquake catalog for the Wasatch fault region. K. E. Sieh and S. K. Singh provided prepublication manuscripts. The manuscript benefitted from constructive reviews by W. J. Arabasz, T. C. Hanks, and K. E. Sieh. D. L. Ahrens, R. Bautista, and R. Cazares were involved in various phases of manuscript preparation, and their hard work is appreciated.

REFERENCES

- Agnew, D. C., and K. E. Sieh, A documentary study of the felt effects of the great California earthquake of 1857, *Bull. Seismol. Soc. Am.*, **68**, 1717-1729, 1978.
- Aki, K., Asperities, barriers, characteristic earthquakes, and strong motion prediction, *J. Geophys. Res.*, this issue.
- Allen, C. R., The tectonic environments of seismically active and inactive areas along the San Andreas fault system, in *Proceedings of the Conference on Geologic Problems of the San Andreas Fault System*, edited by W. R. Dickinson and A. Grantz, *Stanford Univ. Publ. Geol. Sci.*, **11**, 70-82, 1968.
- Anderson, J. G., Estimating the seismicity from geological structure for seismic-risk studies, *Bull. Seismol. Soc. Am.*, **69**, 135-158, 1979.
- Anderson, J. G., Comparison of earthquake occurrence rates in California with predictions based on geological slip rates (abstract), *Eos Trans. AGU*, **64**, 313, 1983.
- Anderson, J. G., and J. E. Luco, Consequences of slip rate constraints on earthquake occurrence relations, *Bull. Seismol. Soc. Am.*, **73**, 471-496, 1983.
- Arabasz, W. J., and R. B. Smith, Earthquake prediction in the Intermountain Seismic Belt; an intraplate extensional regime, in *Earthquake Prediction, An International Review*, edited by D. Simpson and P. Richards, pp. 248-258, AGU, *Maurice Ewing Ser.*, vol. 4, Washington, D. C., 1981.
- Arabasz, W. J., R. B. Smith, and W. D. Richins, Earthquake studies along the Wasatch Front, Utah: Network monitoring seismicity, and seismic hazards, in *Earthquake Studies in Utah, 1850 to 1978*, edited by W. J. Arabasz, R. B. Smith, and W. D. Richins, pp. 253-285, University of Utah Seismograph Stations, Department of Geology and Geophysics, University of Utah, Salt Lake City, 1979.
- Arabasz, W. J., R. B. Smith, and W. D. Richins, Earthquake studies along the Wasatch Front, Utah: Network monitoring seismicity, and seismic hazards, *Bull. Seismol. Soc. Am.*, **70**, 1479-1499, 1980.
- Bakun, W. H., and T. V. McEvilly, Earthquakes near Parkfield, California: Comparing the 1934 and 1966 sequences, *Science*, **205**, 1375-1377, 1979.
- Bakun, W. H., and T. V. McEvilly, Recurrence models and the Parkfield, California, earthquakes, *J. Geophys. Res.*, **89**, 3051-3058, 1984.
- Báth, M., Earthquake recurrence of a particular type, *Pure Appl. Geophys.*, **119**, 1063-1076, 1981.
- Báth, M., Earthquake frequency and energy in Greece, *Tectonophysics*, **95**, 233-252, 1983.
- Bucknam, R. C., Northwestern Utah seismotectonic studies, Summaries of Technical Reports, National Earthquake Hazards Reduction Program, vol. VIII, p. 64, U.S. Geol. Surv., Reston, Va., 1978.
- Davis, T., Late Holocene seismic record, western big bend of the San Andreas fault (abstract), *Geol. Soc. Am. Abstr. Programs*, **13**, 51, 1981.
- Doser, D. I., and R. B. Smith, Seismic moment rates in the Utah region, *Bull. Seismol. Soc. Am.*, **72**, 525-555, 1982.
- Gutenberg, B., and C. F. Richter, *Seismicity of the Earth and Associated Phenomena*, 310 pp., Princeton University Press, Princeton, N. J., 1954.
- Hall, N. T., Holocene history of the San Andreas fault between Crystal Springs Reservoir and San Andreas Dam, San Mateo County, California, *Bull. Seismol. Soc. Am.*, **74**, 281-299, 1984.
- Hintze, L. F., Geologic map of Utah, Utah Geol. and Miner. Surv., Salt Lake City, 1980.
- Klein, J., J. C. Lerman, P. E. Damon, and E. K. Ralph, Calibration of radiocarbon dates: Tables based on the consensus data of the workshop on calibrating the radiocarbon times scales, *Radiocarbon*, **24**, 103-150, 1982.
- Lahr, J. C., and C. D. Stephens, Alaska seismic zone: Possible example of nonlinear magnitude distribution for faults (abstract), *Earthquake Notes*, **53**, 66, 1982.
- Lisowski, M., and W. H. Prescott, Short range distance measurements along the San Andreas fault system in Central California, *Bull. Seismol. Soc. Am.*, **71**, 1607-1624, 1981.
- Molnar, P., Earthquake recurrence intervals and plate tectonics, *Bull. Seismol. Soc. Am.*, **69**, 115-133, 1979.
- Prescott, W. H., M. Lisowski, and J. C. Savage, Geodetic measurement of crustal deformation on the San Andreas, Hayward and Calaveras fault near San Francisco, California, *J. Geophys. Res.*, **86**, 10853-10869, 1981.
- Purcaru, G., A new magnitude-frequency relation for earthquakes and a classification of relation types, *Geophys. J. R. Astron. Soc.*, **42**, 67-79, 1975.
- Real, C. R., T. R. Topozada, and D. C. Parke, Earthquake epicenter map of California, Map Sheet 39, Calif. Div. Mines and Geol., Sacramento, 1978.
- Rust, D. J., Evidence for uniformity of large earthquakes in the "big bend" of the San Andreas fault (abstract), *Eos Trans. AGU*, **63**, 1030, 1982a.
- Rust, D. J., Trenching studies of the San Andreas fault bordering western Antelope Valley, southern California, Summaries of Technical Reports, National Earthquakes Hazards Reduction Program, U.S. Geol. Surv. Open File Rep., 82-840, 89-92, 1982b.
- Rust, D. J., Trenching studies of the San Andreas fault bordering western Antelope Valley, southern California, Summaries of Technical Reports, National Earthquake Hazards Program, U.S. Geol. Surv. Open File Rep., 83-525, 70-71, 1983.
- Schwartz, D. P., K. J. CopperSmith, F. H. Swan III, P. Somerville, and W. U. Savage, Characteristic earthquakes on intraplate normal faults (abstract), *Earthquake Notes*, **52**, 71, 1981.
- Schwartz, D. P., K. L. Hanson, and F. H. Swan III, Paleoseismic investigations along the Wasatch fault zone: An Update, in *Paleoseismicity along the Wasatch Front and Adjacent Areas, Central Utah*, edited by A. J. Crone, *Spec. Stud. Utah Geol. Miner. Surv.*, **62**, 45-49, 1983.
- Scott, W. E., New interpretations of Lake Bonneville stratigraphy and their significance for studies of earthquake hazards assessment along the Wasatch Front, Earthquake Hazards Along the Wasatch and Sierra Nevada Frontal Fault Systems, U.S. Geol. Surv. Open File Rep., 80-801, 548-576, 1980.
- Sharp, R. V., Variable rates of Quaternary strike slip on the San Jacinto fault zone, southern California, *J. Geophys. Res.*, **86**, 1754-1762, 1981.
- Sieh, K. E., A study of late Holocene displacement history along the south-central reach of the San Andreas fault, Ph.D. dissertation, 219 pp., Stanford Univ., Stanford, Calif., 1977.
- Sieh, K. E., Slip along the San Andreas fault associated with the great 1857 earthquake, *Bull. Seismol. Soc. Am.*, **68**, 1421-1448, 1978a.
- Sieh, K. E., Central California foreshocks of the great 1857 earthquake, *Bull. Seismol. Soc. Am.*, **68**, 1731-1749, 1978b.
- Sieh, K. E., A review of geological evidence for recurrence times of large earthquakes, in *Earthquake Prediction, An International Review, Maurice Ewing Ser.*, vol. 4, edited by D. W. Simpson and P. G. Richards, pp. 181-207, AGU, Washington, D. C., 1981.
- Sieh, K. E., Aspects of the Holocene history and behavior of the San Andreas fault system, Summaries of Technical Reports, National Earthquake Hazards Reduction Program, U.S. Geol. Surv. Open File Rep., 83-90, 160-162, 1983.
- Sieh, K. E., Lateral offsets and revised dates of large prehistoric earthquakes at Pallett Creek, southern California, *J. Geophys. Res.*, in press, 1984.
- Sieh, K. E., and R. H. Jahns, Holocene activity of the San Andreas fault at Wallace Creek, California, *Geol. Soc. Am. Bull.*, in press, 1984.

- Singh, S. K., L. Astiz, and H. Havskov, Seismic gaps and recurrence periods of large earthquakes along the Mexican subduction zone: A reexamination, *Bull. Seismol. Soc. Am.*, 71, 827-843, 1981.
- Singh, S. K., M. Rodriguiz, and L. Esteva, Statistics of small earthquakes and frequency of occurrence of large earthquakes along the Mexican subduction zone, *Bull. Seismol. Soc. Am.*, 73, 1779-1796, 1983.
- Slemmons, D. B., State-of-the-art for assessing earthquake hazards in the United States, Report 6, Faults and earthquake magnitude, *Misc. Pap. S-73-1*, pp. 1-129, U.S. Army, Corps of Eng., Waterways Exp. Stn., Vicksburg, Miss., 1977.
- Smith, R. B., Seismicity and earthquake hazards of the Wasatch front, Utah, *Earthquake Inf. Bull.*, 6, 12-17, 1974.
- Smith, R. B., and R. L. Bruhn, Intraplate extensional tectonics of the eastern Basin and Range: Inferences on structural style from seismic reflection data, regional tectonics, and thermal-mechanical models of brittle-ductile deformation, *J. Geophys. Res.*, this issue.
- Snay, R. A., R. B. Smith, and T. Soler, Horizontal strain across the Wasatch front near Salt Lake City, Utah, *J. Geophys. Res.*, 89, 1113-1122, 1984.
- Swan, F. H., III, D. P. Schwartz, and L. S. Cluff, Recurrence of moderate to large magnitude earthquakes produced by surface faulting on the Wasatch fault, Utah, *Bull. Seismol. Soc. Am.*, 70, 1431-1462, 1980.
- Swan, F. H., III, K. L. Hanson, D. P. Schwartz, and P. L. Knuepfer, Study of earthquake recurrence intervals on the Wasatch fault at the Little Cottonwood Canyon site, Utah, *U.S. Geol. Surv. Open File Rep.*, 81-450, 30 pp., 1981.
- Thatcher, W., J. A. Hileman, and T. C. Hanks, Seismic slip distribution along the San Jacinto fault zone, southern California, and its implications, *Geol. Soc. Am. Bull.*, 86, 1140-1146, 1975.
- Topozada, T. R., C. R. Real, S. P. Bezore, and D. L. Parke, Preparation of isoseismal maps and summaries of reported effects for pre-1900 California earthquakes, *Open File Rep. OFR 80-15 SAC*, 78 pp., Calif. Div. of Mines and Geol., Sacramento, 1980.
- Wallace, R. E., Earthquake recurrence intervals on the San Andreas fault, *Geol. Soc. Am. Bull.*, 81, 2875-2890, 1970.
- Wallace, R. E., Map of fault scarps formed during earthquake of October 2, 1915, Pleasant Valley, Nevada, and other young fault scarps, *U.S. Geol. Surv. Open File Rep.*, 80-608, 1980.
- Weldon, R. J., and K. E. Sieh, Holocene rate of slip along the San Andreas fault and related tilting near Cajon Pass, southern California (abstract), *Geol. Soc. Am., Abstr. Programs*, 12, 159, 1980.
- Wesnousky, S., C. H. Scholz, K. Shimazaki, and T. Matsuda, Earthquake frequency distribution and the mechanics of faulting, *J. Geophys. Res.*, 88, 9331-9340, 1983.
- Zandt, G., and T. J. Owens, Crustal flexure associated with normal faulting and implications for seismicity along the Wasatch Front, Utah, *Bull. Seismol. Soc. Am.*, 70, 1501-1520, 1980.
- Zoback, M. L., Structure and Cenozoic tectonism along the Wasatch fault zone, Utah, *Mem. Geol. Soc. Am.*, 157, 3-27, 1983.

K. J. CopperSmith and D. P. Schwartz, Woodward-Clyde Consultants, One Walnut Creek Center, 100 Pringle Avenue, Walnut Creek, CA 94596.

(Received October 24, 1983;
revised March 21, 1984;
accepted April 10, 1984.)